

Astaxanthin attenuates diabetic kidney injury through upregulation of autophagy in podocytes and pathological crosstalk with mesangial cells

Mengqi Hong^{a,b#}, Zhenyu Nie^{b#}, Zhengyue Chen^b and BeiYan Bao^b

^aNingbo Ninth Hospital, Ningbo City, Zhejiang, China; ^bDivision of Nephrology, Ningbo Urology and Nephrology Hospital, Ningbo City, Zhejiang, China This is an Open Access article distributed under the terms of the Creative Commons Attribution License (<http://creativecommons.org/licenses/by/4.0/>), which permits unrestricted use, distribution, and reproduction in any medium, provided the original work is properly cited. The terms on which this article has been published allow the posting of the Accepted Manuscript in a repository by the author(s) or with their consent.

ABSTRACT

Objectives: Astaxanthin (ATX) is a strong antioxidant drug. This study aimed to investigate the effects of ATX on podocytes in diabetic nephropathy and the underlying renal protective mechanism of ATX, which leads to pathological crosstalk with mesangial cells.

Methods: In this study, diabetic rats treated with ATX exhibited reduced 24-h urinary protein excretion and decreased blood glucose and lipid levels compared to vehicle-treated rats. Glomerular mesangial matrix expansion and renal tubular epithelial cell injury were also attenuated in ATX-treated diabetic rats compared to control rats.

Results: ATX treatment markedly reduced the α -SMA and collagen IV levels in the kidneys of diabetic rats. Additionally, ATX downregulated autophagy levels. *In vitro*, compared with normal glucose, high glucose inhibited LC3-II expression and increased p62 expression, whereas ATX treatment reversed these changes. ATX treatment also inhibited α -SMA and collagen IV expression in cultured podocytes. Secreted factors (vascular endothelial growth factor B and transforming growth factor- β) generated by high glucose-induced podocytes downregulated autophagy in human mesangial cells (HMCs); however, this downregulation was upregulated when podocytes were treated with ATX.

Conclusions: The current study revealed that ATX attenuates diabetes-induced kidney injury likely through the upregulation of autophagic activity in podocytes and its antifibrotic effects. Crosstalk between podocytes and HMCs can cause renal injury in diabetes, but ATX treatment reversed this phenomenon.

ARTICLE HISTORY

Received 4 April 2024

Revised 16 June 2024

Accepted 7 July 2024

KEYWORDS

Astaxanthin; diabetic nephropathy; podocytes; autophagy; crosstalk; mesangial cells


1. Introduction

Diabetic nephropathy (DN) is one of the main causes of end-stage kidney disease (ESKD) in patients with diabetes mellitus (DM) [1,2]. Currently, there are 100 million diabetic adults and 150 million prediabetic patients in China [3,4]. Chronic kidney disease (CKD) is estimated to affect 120 million people in China [5]. The glomerulus is an early and important site of diabetic injury in the kidney. Glomerular hypertrophy, basement membrane thickening, capillary loop obliteration, and the loss of podocytes from the glomerular filtration barrier are hallmarks of progressive DN, and the degree of podocyte loss correlates with disease severity [6]. Progressive podocyte injury, characterized by low podocyte density and number, hypertrophy, and foot process effacement, plays a central role in the development of DN in both type 1 and type 2 diabetes patients [7]. Therefore, podocyte damage is a key factor that can be used as a clinical predictor of DN progression. Mesangial cells are the primary cell type in the glomeruli. Abnormal activation of mesangial cells

plays an important role in the pathogenesis of diabetic glomerulosclerosis. Podocytes are connected by special intercellular junctions called septa and are separated from the endothelial lumen by the basement membrane of the glomerulus. For this structure to function, these cells must cross-communicate with each other. It has been reported that glomerular podocytes and endothelial cells, endothelial cells and mesangial cells, and podocytes and mesangial cells communicate with each other. However, the molecular mechanisms underlying glomerular cell crosstalk and feedback regulation in proteinuric glomerular diseases are poorly understood. In particular, direct *in vivo* evidence of communication between podocytes and mesangial cells is scarce [8]. Currently, several signaling pathways, including those involving endothelin-1, chemokine C-C motif receptor 7 and its ligand SLC/CCL21, platelet-derived growth factor, connective tissue growth factor, hepatocyte growth factor, and transforming growth factor- β (TGF- β), have been suggested to be involved in this type of signaling [8].

CONTACT Zhengyue Chen  yilanczy2019@163.com BeiYan Bao  baobeiyan2007@sina.com  Division of Nephrology, Ningbo Urology and Nephrology Hospital, 998 Qianhe North Road, Ningbo City 315192, Zhejiang, China

[#]These authors contributed equally to this work

 Supplemental data for this article can be accessed online at <https://doi.org/10.1080/0886022X.2024.2378999>.

© 2024 The Author(s). Published by Informa UK Limited, trading as Taylor & Francis Group

This is an Open Access article distributed under the terms of the Creative Commons Attribution-NonCommercial License (<http://creativecommons.org/licenses/by-nc/4.0/>), which permits unrestricted non-commercial use, distribution, and reproduction in any medium, provided the original work is properly cited. The terms on which this article has been published allow the posting of the Accepted Manuscript in a repository by the author(s) or with their consent.

Autophagy is a lysosome-dependent mass degradation process that is highly conserved from yeasts to mammals. Autophagy typically participates in the elimination of long-term aggregated and misfolded proteins, damaged and excessive organelles, and intracellular pathogens [9]. Autophagy is primarily responsible for the destruction of proteins and organelles after the regulation of cellular homeostasis and is considered to be an essential inducing factor of posttranslational damage [10]. Numerous signaling molecules are involved in autophagy. Studies have suggested that the alteration of nutrient-sensing pathways under diabetic conditions impairs the autophagic stress response, which may exacerbate organelle dysfunction and lead to DN development [11]. Thus, autophagy represents a potential therapeutic target for treating DN caused by cell damage [12].

Astaxanthin (3,3'-dihydroxy-B, B'-carotenoids 4,4'-dione, ATX) is called 'marine carotenoid', and ATX has stronger antioxidant activity than other carotenoids and relies on the quenching of free radicals. These compounds are widespread in marine organisms such as algae, crustaceans, salmon, prawns, and crabs [13,14]. Previous research has demonstrated that ATX protects against hepatic damage [15,16], neurological activity [17], and cardiovascular damage [18]. ATX also prevents oxidative stress, inflammatory reactions, and apoptosis in patients with DM [19,20]. It has been demonstrated that ATX attenuates both lung and liver fibrosis [21,22]. However, the effect of ATX on renal fibrosis has not yet been explored, and it is unclear whether ATX can ameliorate renal fibrosis by regulating autophagy. In this study, streptozotocin (STZ) injection and a high-fat (HF) diet were used to induce renal fibrosis in DN rats *in vivo*; these rats along with *in vitro* high glucose-induced human podocytes were used to investigate the effect of ATX on renal fibrosis in DN and its potential protective mechanisms. Supernatant transfer experiments were also used to investigate how podocytes release signaling factors through autophagy to induce mesangial cell autophagy, which further improves renal fibrosis.

2. Materials and methods

2.1. Materials

ATX was obtained from Shanghai Second Military Medical University. Antibodies against α -SMA (ab5694, Abcam, USA), collagen IV (ab6586, Abcam, USA), p62 (ab109012, Abcam, USA), LC3-II/LC3-I (14600-1-AP, Proteintech, China), and StubRFP-sensGFP-LC3 were obtained from GeneChem (China).

2.2. Animals and experimental design

Thirty male 8-week-old Sprague–Dawley (SD) rats (250–300 g) were purchased from the Experimental Animal Center of Zhejiang Province (Zhejiang, Certificate No.0012371). Rats were housed in an SPF-grade laboratory animal room at the Animal Laboratory Center of Ningbo University with a room temperature of approximately 25°C, 50%–60% humidity, and

a 12h light/dark cycle. The standard diet was provided by the Animal Laboratory Center of Ningbo University, and the HF diet was purchased from Pu Luteng Bio-Technique Co., Ltd. The HF diet (HFD) contained 16.9% fat and 10.2% casein compared to the standard diet. The Research Ethics Committee of Ningbo University, China, approved the experimental protocol (AEWC-20140127).

Each rat was fed a HF diet (30 g/day) for eight weeks to induce insulin resistance. The diabetic model was generated by intraperitoneal injection of STZ (diluted to 1% in 10 mmol/L citrate buffer, pH 4.5) at 25 mg/kg body weight (BW) after the rats had fasted for 12 h [20]. Rats in the normal group were injected with an equal volume of citrate buffer. Blood glucose was measured 72 h after STZ injection, and rats with blood glucose levels greater than 16.7 mmol/L were considered diabetic [21]. Rats were fed a HF diet, except for those in the normal group, to maintain high blood glucose levels.

Thirty male rats were randomly divided into the following five groups: (1) the normal group (NG), which was fed a standard diet for 15 weeks; (2) the HF group, which was fed a high-fat diet for 15 weeks, gavaged with normal saline during the 7th–9th weeks, and injected with citrate buffer; and (3) the HF diet plus ATX prevention group (HA), which was fed a high-fat diet for 15 weeks and gavaged with ATX (25 mg/kg BW/day) during the 7th–9th weeks and injected with citrate buffer; (4) the DM group, fed a high-fat diet for 15 weeks, gavaged with normal saline during the 7th–9th weeks and injected with STZ; 5) the DM plus ATX prevention group (DA), fed a high-fat diet for 15 weeks and gavaged with ATX (25 mg/kg BW/day) during the 7th–9th weeks and injected with STZ. The susceptibility of beta islet cells to STZ increased in rats fed a HF diet (Figure 1A). Hence, whether HF rats had metabolic disorders or renal injury was assessed in the HF group, and whether ATX had an impact on these changes was confirmed in the HA group.

2.3. Measurement of body weight, blood glucose, urinary protein and other biochemical parameters

Body weight (BW) was measured once a month. At the end of the study, blood glucose was measured using a glucometer (Lifescan One Touch Ultra) with samples obtained from the tail vein of the rats. Fasting blood glucose (FBG) was measured after 12 h of fasting, and postprandial blood glucose (PBG) was measured 2 h after a meal. Blood glucose levels were determined using One Touch Ultra test strips and a blood glucose meter (Johnson & Johnson Medical Ltd., Shanghai, China). The oral glucose tolerance test (OGTT) was performed on overnight-fasted rats at the end of the study. Rats were fasted for 12 h and then given a glucose solution (2 g/kg BW), and blood samples were collected before and 2 h after the glucose solution was given. Serum insulin levels were measured using a rat insulin ELISA kit (Qiaodu, Shanghai, China). Clinically, renal involvement in patients with diabetes is defined by the appearance of microalbuminuria at an early stage. Microalbuminuria is considered a marker of DN progression to ESKD [23]. The

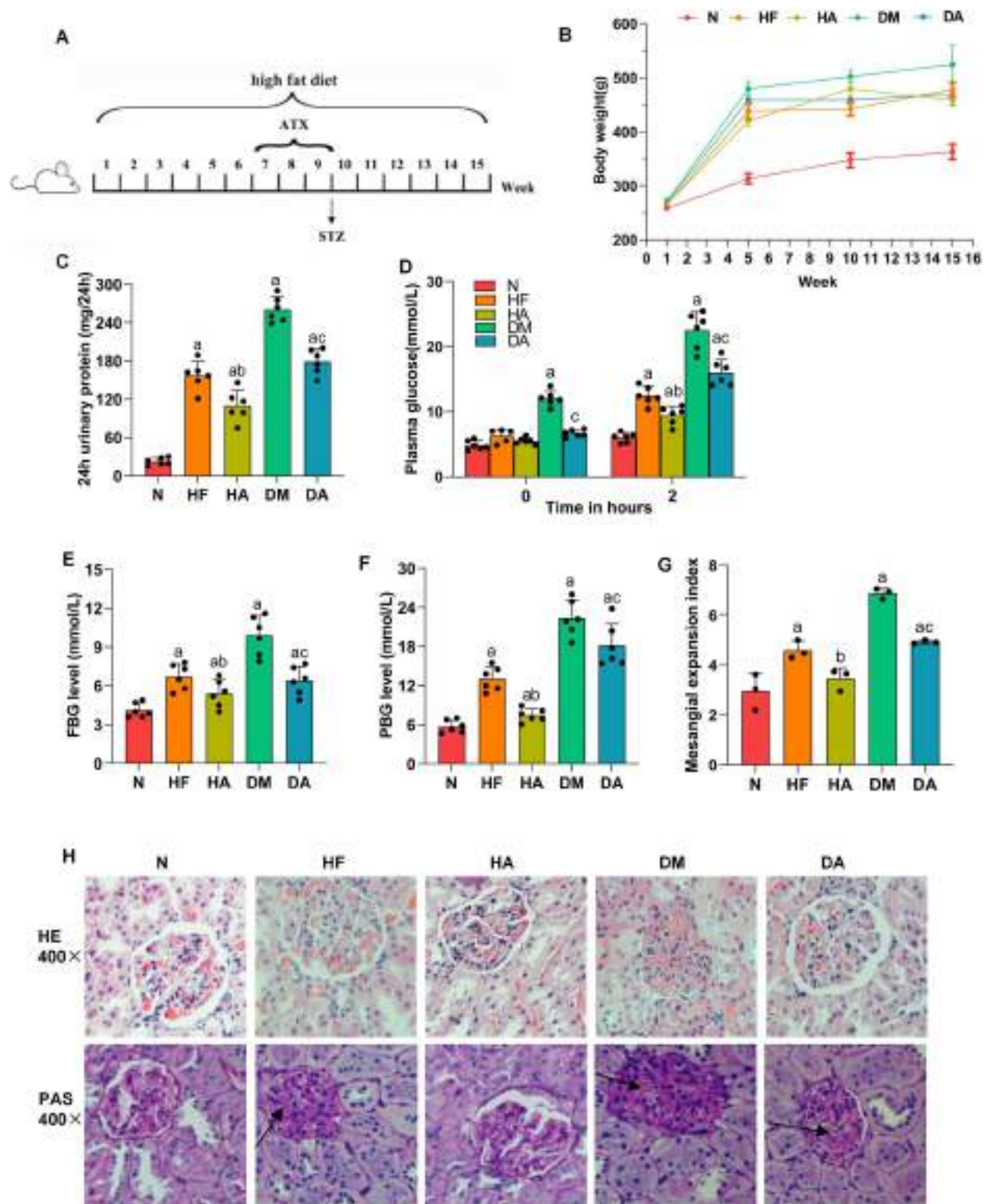


Figure 1. Astaxanthin decreased body weight, biochemical parameters, and renal injury according to pathology. (A) schematic of the 15-week group design. (B) Astaxanthin decreased body weight each month in HFD-fed and diabetic rats. (C) Astaxanthin decreased 24-h urinary protein at the end of the study in HFD-fed and diabetic rats. (D) Astaxanthin decreased plasma glucose at 0h and 2h in HFD-fed and diabetic rats. (E) Astaxanthin decreased FBG levels at the end of the study in HFD-fed and diabetic rats. (F) Astaxanthin decreased PBG levels at the end of the study in individuals with a high fat diet and diabetes. (G) semiquantification of PAS staining. (H) HE staining and PAS staining showed that astaxanthin treatment alleviated renal injury in HFD-fed and diabetic rats. The results are presented as the mean \pm SD, $n \geq 3$. $^a p < 0.05$ compared with the normal group, $^b p < 0.05$ compared with the HF group, $^c p < 0.05$ compared with the DM group.

rats were housed individually in metabolic cages for 24h to collect urine samples, which were then analyzed using a MODULAR P800 Automation Biochemist Analyzer (Roche,

Basel, SWIT). At the end of the experiment, serum samples were collected to detect high-density lipoprotein cholesterol (HDL-C), low-density lipoprotein cholesterol (LDL-C),

total cholesterol (TC), triglyceride (TG), urea nitrogen (BUN), creatinine (CREA), and uric acid (UA) levels. These biochemical indicators were measured using the MODULAR P800 Automation Biochemist Analyzer (Roche, Basel, SWIT). Finally, the rats were sacrificed, and kidney tissues were removed from the rats.

2.4. Histological and immunohistochemical staining

The peripheral part (more renal cortex) of the kidney was fixed in 4% formaldehyde, dehydrated, and embedded in paraffin. Tissue sections (3 μ m) were stained with hematoxylin and eosin (H&E) and periodic acid-Schiff (PAS) and observed under a light microscope. Renal slides were subjected to immunohistochemical staining of α -SMA and collagen IV with the following primary antibodies: monoclonal mouse anti-rat α -smooth muscle actin (α -SMA) (1:50 dilution) and polyclonal rabbit anti-rat collagen IV (1:200 dilution). The sections were then incubated with horseradish peroxidase-labeled secondary antibodies (1:1000) for 30 min. The sections were incubated with diaminobenzidine (DAB; Boster, China) and counterstained with hematoxylin. The mesangial expansion index was defined as the percentage of the positive area of the entire glomerulus. Quantitative analysis of brown positive staining in the glomerulus and tubules was performed using Image-Pro Plus 6.0 (Media Cybernetics, USA).

2.5. Cell culture

Immortalized human podocytes were kindly provided by Professor Cijiang He (Mount Sinai School, UK). Human podocytes were cultured in RPMI 1640 medium supplemented with 10% fetal bovine serum (FBS; Gibco, USA). Human podocytes were incubated at 33°C with the addition of 1% insulin-transferrin-selenium (Life Technologies). After reaching 50% - 60% confluency, the cells were transferred to 37°C to stop proliferation and achieve full differentiation within 14 days. The cells were pretreated with ATX at concentrations of 2, 10, or 25 μ g/mL for 24 h. The primary cells were divided into six groups: (1) the normal group (NG, no treatment (D-glucose 5.5 mmol/L)); (2) ATX prevention group (NG+ATXM, treatment with ATX diluted in 5.5 mmol/L D-glucose at a concentration of 10 μ g/mL); (3) high glucose group (HG, treatment with 30 mmol/L D-glucose); (4) ATX low group (HG+ATXL, treatment with ATX diluted in 30 mmol/L D-glucose at a concentration of 2 μ g/mL); (5) ATX medium group (HG+ATXM, treatment with ATX diluted in 30 mmol/L D-glucose at a concentration of 10 μ g/mL); and (6) ATX high group (HG+ATXH, treatment with ATX diluted in 30 mmol/L D-glucose at a concentration of 25 μ g/mL).

Human mesangial cells (HMCs) were cultured in RPMI-1640 supplemented with 10% FBS, 100 U/mL penicillin, and 0.1 mg/mL streptomycin at 37°C in a humidified atmosphere containing 5% CO₂. The primary cells were divided into four groups: (1) the control group (Ctrl, no treatment); (2) the control group (P(Ctrl), which was incubated with the supernatant derived from podocytes treated with 5.5 mmol/L

D-glucose for 24 h); (3) the high glucose group (P(HG), which was incubated with the supernatant derived from podocytes treated with 30 mmol/L D-glucose for 24 h); and (4) the high glucose group and ATX group (P(HG+ATX), which was incubated with the supernatant derived from podocytes treated with 30 mmol/L D-glucose and 10 μ g/mL ATX for 24 h).

2.6. qRT-PCR analysis of gene expression in renal tissues

Total RNA was extracted from renal tissues using TRIzol reagent (Invitrogen, USA). One microgram of total RNA was reverse transcribed. Polymerase chain reaction was performed in a LightCycler 480 II Authorized Thermal Cycler (Roche, Basel, SWIT) using the following protocol: denaturation at 95°C for 5 min, followed by 45 cycles of 95°C for 10 s, annealing for 20 s, and 72°C for 30 s. The primer sequences were as follows: Rat/Human β -actin, forward: 5'-CACGAACTACCTTCAACTCC-3', reverse: 5'-CATACTCCTGCTTGCTGATC-3'; Rat α -SMA, forward: 5'-GCGTGGCTATTCTTCGTGACTAC-3', reverse: 5'-CCATCAGGCAGTTCGTAGCTC TTC-3'; Rat collagen IV, forward: 5'-CCATCTGTGGACCATGGCTT-3', reverse: 5'-GCGAAGTTGCAGACGTTGTT-3'; Human α -SMA, forward: 5'-CGGACAGCGCCAAGTGAAG-3', reverse: 5'-TTGTGTCTAGTTTCTGGGCGG-3'; and Human collagen IV, forward: 5'-GGA TAACAGGCGTGACTGGAGT-3', reverse: 5'-CTTTGCCACCAGGCAGTCCAAT-3'. Relative mRNA levels were determined using the 2^{- $\Delta\Delta$ Ct} method, with the β -actin gene serving as the internal reference.

2.7. Enzyme-linked immunosorbent assay (ELISA) and western blot analysis

The concentrations of vascular endothelial growth factor B (VEGF-B) and TGF- β 2 in the podocyte supernatants were measured using ELISA kits (Abcam, Cambridge, MA, USA) according to the manufacturer's instructions. The concentrations were calculated using the appropriate optical density values.

Renal tissues were dissected and homogenized in radio-immunoprecipitation assay (RIPA) buffer (Solarbio, Beijing, China). Podocytes were washed twice with PBS and lysed using RIPA buffer. The samples were separated by 8% sodium dodecyl sulfate-polyacrylamide gel electrophoresis and transferred to polyvinylidene fluoride membranes. The membranes were blocked with Tris-buffered saline (TBS) solution (25 mM Tris-HCl, 150 mM NaCl, pH = 7.4) supplemented with 5% nonfat dried milk for 1 h and then incubated overnight with primary antibodies against β -actin (1:1000), α -SMA (1:400), collagen IV (1:1000), LC3-II/I (1:5000), and p62 (1:1000) at 4°C. The membranes were then incubated with an HRP-labeled secondary antibody (Beyotime, China) for 60 min. The immunoreactions were visualized with an enhanced chemiluminescence (ECL) developer solution and detected using a gel imaging and analysis system (Tanon, Shanghai, China). The density values of the bands were quantified using ImageJ software (NIH, Maryland, USA).

2.8. Evaluation of fluorescent LC3 puncta

Cells cultured on coverslips were transfected with an adenovirus containing fluorescent mRFP-GFP-LC3 (Hanbio, Inc., Shanghai, CN), a specific marker for autophagosome formation. After adenoviral transfection for 48h, the cells were fixed with 4% paraformaldehyde after treatment with 5.5mmol/L D-glucose or 10μg/ml ATX. Images of the cells were obtained with a confocal laser scanning microscope (Nikon, A1 PLUS, Tokyo, Japan) and analyzed using ImageJ software. Cells were detected with green (GFP) or red (mRFP) fluorescence.

2.9. Statistics

The data are presented as the mean±standard deviation (SD). The differences among the groups were analyzed using a randomized block design analysis of variance with the Statistical Package for Social Sciences (SPSS) software (version 22.0). Differences were considered statistically significant at $p < 0.05$.

3. Results

3.1. Effects of astaxanthin on body weight, biochemical parameters, and renal injury pathology

All rats were alive at the end of the study. As displayed in Figure 1B, BW was significantly greater in the HF, HA, DM, and DA groups from the 1st - 15th weeks than in the normal group. At the end of the 15th week, the BW in the HA group was lower than that in the HF group, and the BW in the DA group was lower than that in the DM group. The 24-h urinary protein level was significantly greater in all groups than in the normal group. Moreover, the urinary protein levels in the DA group were lower than those in the DM group. Similarly, the urinary protein levels in the HA group were lower than those in the HF group (Figure 1C). Figure 1D shows that in the OGTT, blood glucose in the normal group was lower than that in the HF, HA, DM and DA groups. However, compared to those in the HF and DM groups, the blood glucose levels in the HA and DA groups were lower. FBG and PBG levels were measured at the end of the study. The rats in the HF, DM, and DA groups had higher FBG and PBG levels than did those in the normal group. However, the FBG and PBG levels in the HA group were lower than those in the HF group, and the DA group

had lower levels of FBG and PBG than did the DM group (Figure 1E, F). This finding could be because ATX effectively prevented an increase in serum glucose in the model group, showing that ATX effectively attenuated blood glucose levels in HF diet-fed and diabetic rats. As shown in Table 1, compared to those in the normal group, the HDL-C, LDL-C, TC, TG, BUN, and UA levels in the HF, HA, DM, and DA groups were significantly different. LDL-C, TC, TG, BUN, and UA levels were significantly increased, whereas HDL-C levels were significantly decreased. However, LDL-C, TC, BUN and UA levels were substantially lower in the DA group than in the DM group, and HDL-C levels were significantly increased. The LDL-C, TC, TG and UA levels in the HA group were significantly lower than those in the HF group, whereas the HDL-C level was significantly greater. These data indicate that oral ATX may decrease lipid metabolism as well as urea nitrogen and uric acid levels. As shown by the black arrow in the pathological staining figure, the glomeruli in the HF and DM groups were larger in volume, accompanied by tubular epithelial swelling. Renal injury was more severe in the DM group compared with the HF group. However, ATX treatment reversed this effect in the kidneys of HF and DM rats (Figure 1G, H). These findings suggested that ATX treatment has an antifibrotic effect on diabetic nephropathy.

3.2. Astaxanthin alleviated renal fibrosis in rats

Next, α-SMA and collagen IV mRNA and protein levels were evaluated in the renal tissues of rats in all experimental groups. Compared to those in the normal group, α-SMA and collagen IV expression was significantly greater in the HF and DM groups. Compared with those in the HF and DM groups, the HA and DA groups treated with ATX exhibited significantly reduced α-SMA and collagen IV expression (Figure 2A–E). As shown in Figure 2F, immunohistochemical analysis revealed an increase in both α-SMA and collagen IV protein expression in the DM group; however, this increase decreased after ATX treatment. These data suggest that ATX decreases α-SMA and collagen IV mRNA and protein levels in diabetic rats, thus alleviating renal injury.

3.3. Astaxanthin upregulated autophagy in the renal tissues of rats and podocytes

LC3 and P62 are important autophagy markers. To elucidate the mechanism by which ATX promotes autophagy, the

Table 1. Biochemical parameters for all rats at the end of the study.

	N	HF	HA	DM	DA
HDL-C (mmol/mL)	1.71 ± 0.10	1.26 ± 0.58 ^a	1.41 ± 0.10 ^{ab}	1.14 ± 0.02 ^a	1.01 ± 0.04 ^{ac}
LDL-C (mmol/mL)	0.44 ± 0.12	0.67 ± 0.14 ^a	0.60 ± 0.03 ^{ab}	0.74 ± 0.07 ^a	0.59 ± 0.03 ^{ac}
TC (mmol/mL)	1.26 ± 0.12	2.27 ± 0.15 ^a	1.83 ± 0.22 ^{ab}	2.81 ± 0.37 ^a	1.94 ± 0.07 ^{ac}
TG (mmol/mL)	0.68 ± 0.11	3.33 ± 0.62 ^a	2.40 ± 0.10 ^{ab}	4.61 ± 0.97 ^a	3.87 ± 0.64 ^a
BUN (μmol/L)	3.90 ± 0.91	5.55 ± 0.38 ^a	4.96 ± 0.55 ^a	6.38 ± 0.25 ^a	5.79 ± 0.18 ^{ac}
CREA (μmol/L)	19.33 ± 5.39	22.00 ± 2.10	20.83 ± 2.32	22.50 ± 1.38	19.50 ± 4.37
UA (μmol/L)	73.83 ± 5.00	139.67 ± 17.22 ^a	119.50 ± 12.72 ^{ab}	203.00 ± 28.81 ^a	142.17 ± 25.62 ^{ac}

Results are presented as mean±SEM, $n=6$. ^a $p < 0.05$ compared with the normal group, ^b $p < 0.05$ compared with the HF group, ^c $p < 0.05$ compared with the DM group.

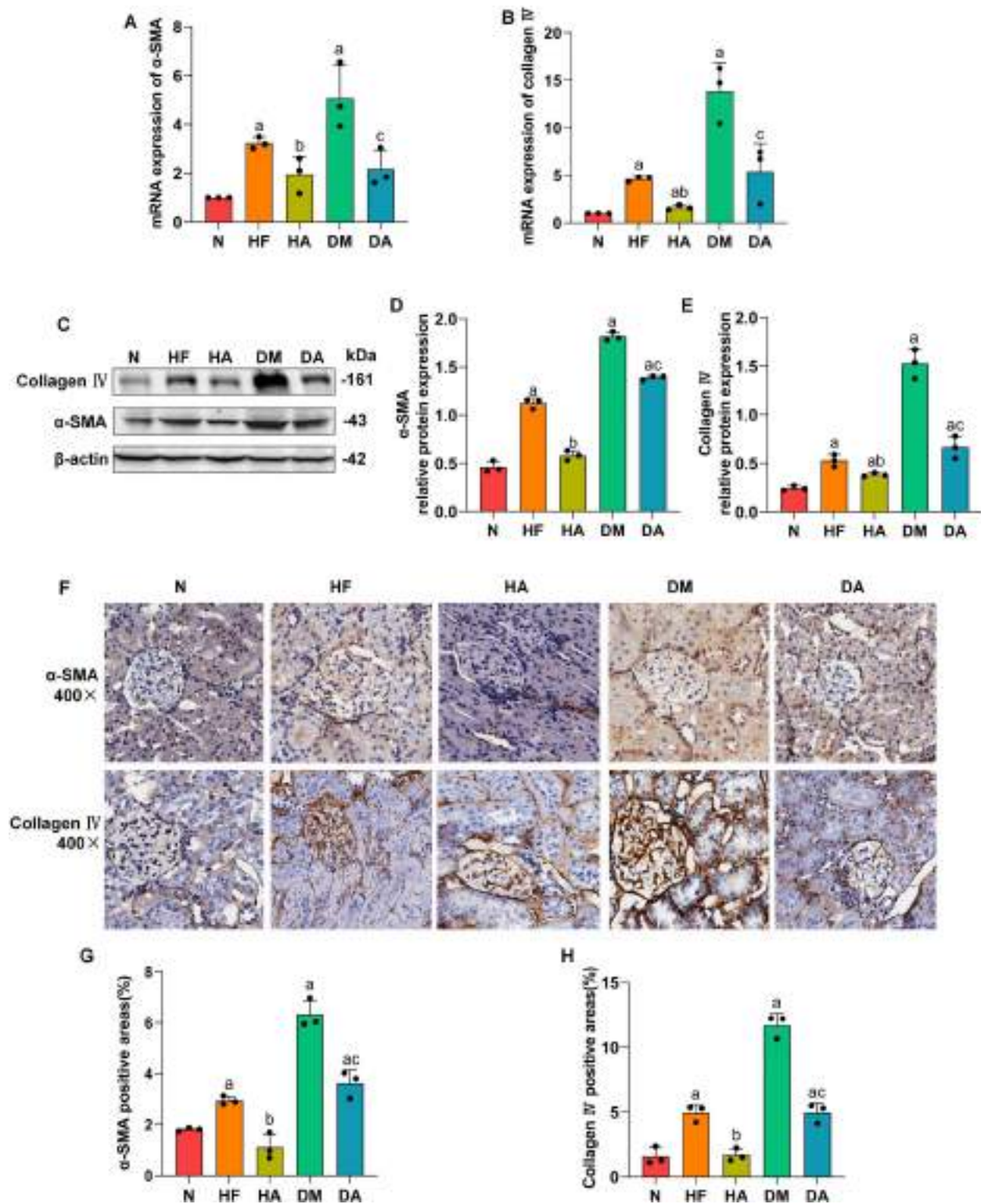


Figure 2. Astaxanthin treatment reduced α -SMA and collagen IV expression in the kidneys of rats. (A, B) α -SMA and collagen IV mRNA expression was determined using real-time PCR; $n \geq 3$. (C, D, E) α -SMA and collagen IV protein expression was determined using Western blotting; $n \geq 3$. (F) immunohistochemical analysis of α -SMA and collagen IV protein expression by immunohistochemistry. The results are presented as the mean \pm SD, ^a $p < 0.05$ compared with the normal group, ^b $p < 0.05$ compared with the HF group, ^c $p < 0.05$ compared with the DM group.

relative expression levels of the autophagy pathway-related proteins LC3-II/I and p62 were detected using western blotting. LC3-II/I levels were significantly lower and p62 levels were significantly greater in the HF and DM groups than in

the normal group. After treatment with ATX, p62 protein levels were significantly greater in rats in the DM group than in those in the DA group. Conversely, the LC3-II/I ratio was lower in the rats in the HA and DA groups than in those in

the HF and DM groups (Figure 3A–C). As shown in Supplementary Figure 1A, compared to those in the DM group, there were fewer sedimentary heparin granules in the DM+rapamycin group. These data indicate that ATX protects against renal injury by increasing autophagy in diabetic rats.

The regulation of renal autophagy by ATX was also investigated *in vitro*. Figure 3D–F show that the LC3-II/I ratio markedly increased with ATX treatment at 2, 10, and 25 $\mu\text{g/mL}$ in cells cultured in 30 mmol/L D-glucose for 24 h compared to that in the high glucose group without ATX. Furthermore, compared to the ratios at other concentrations, the LC3-II/I ratio was highest in the group treated with 25 $\mu\text{g/mL}$ ATX. The p62 protein level was significantly greater in the HG group compared with the normal group and was lower at 2 and 10 $\mu\text{g/mL}$ in cells cultured in 30 mmol/L D-glucose than in the high glucose group. Conversely, no significant differences were observed in the relevant LC3-II/I and p62 indicators between the NG and NG+ATXM groups. Next, we analyzed autophagic flux with immunoblotting for endogenous LC3. ATX (10 $\mu\text{g/mL}$) was used to treat cells cultured in 30 mmol/L D-glucose. The results showed that the autophagy of podocytes was rapidly inhibited by high glucose treatment; however, compared to that in the high glucose group, the number of LC3 fluorescent puncta was significantly increased by ATX treatment for 24 h (Figure 3G).

Further evaluation of the effect of ATX on the regulation of fibrosis factors in podocytes revealed that α -SMA and collagen IV expression in podocytes was significantly upregulated after 24 h of culture under high-glucose conditions. However, compared with those in the HG group, α -SMA and collagen IV mRNA and protein expression levels were significantly lower in the ATX treatment group (2, 10, and 25 $\mu\text{g/mL}$). By comparing ATX at three different concentrations, we found that α -SMA mRNA and protein expression levels were the lowest after treatment with 2 $\mu\text{g/mL}$ ATX, and collagen IV mRNA and protein expression levels were the lowest after treatment with 10 $\mu\text{g/mL}$ ATX. We also found that compared with those in the NG and NG+ATXM groups, α -SMA and collagen IV expression in the NG+ATXM groups was decreased (Figure 3H–L). This finding suggested that ATX may also protect normal podocytes against fibrosis. These results indicated that ATX blocked the inhibitory effect of 30 mmol/L D-glucose on podocytes at the autophagy level.

3.4. Complex intercellular communication networks in podocytes and mesangial cells in diabetic nephropathy

The scRNA-seq data were downloaded from the Gene Expression Omnibus database. In total, nine clusters were identified after UMAP dimensionality reduction. The marker genes of these nine clusters were obtained from the cell marker database (Figure 4A, B). Furthermore, pathways involved in podocyte activation in DN include the mitogen-activated protein kinase (MAPK) signaling pathway, autophagy pathway, phosphatidylinositol 3-kinase/protein kinase B (PI3K-Akt) signaling pathway, and regulation of the actin cytoskeleton (Figure 4D). As shown in Figure 4C, VEGF- β ,

TGF- β 2, and tumor necrosis factor receptor superfamily 10 (TNFSF10) strongly interact with podocytes and mesangial cells in DN. Autophagy is involved in regulating VEGF during high glucose-induced podocyte injury [24]. Another study showed that autophagy inhibition triggers a cell-autonomous fibrogenic impairment linked to profound remodeling of the TGF-BMP signaling gene program [25]. Therefore, we hypothesize that podocytes secrete VEGF-B and TGF- β 2 by regulating autophagy, thereby affecting mesangial cell autophagy in a high-glucose environment. The ELISA results revealed that the high glucose-stimulated expression of VEGF-B and TGF- β 2 was significantly increased in the supernatants of podocytes. VEGF-B and TGF- β 2 expression was significantly decreased in the supernatants of podocytes treated with ATX (Figure 5A, B).

3.5. Podocyte autophagy results in the secretion of factors into the supernatant that affect mesangial cell autophagy

The mesangial cells showed a significant increase in collagen IV protein expression in the HG group relative to that in the NG group. However, compared with that in the HG group, collagen IV protein expression in the HG+ATX group was not significantly different (Supplementary Figure 1B). Crosstalk between autophagy in HMCs and podocytes was then investigated by analyzing autophagy in the Ctrl, P(Ctrl), P(HG), and P(HG+ATX) groups. As shown in Figure 5C–G, compared to that in the P(Ctrl) group, autophagy in the HMCs was significantly decreased when the HMCs were incubated with the supernatant derived from podocytes treated with high glucose. Compared to that in the P(HG) group, HMC autophagy was significantly greater in the P(HG+ATX) group. Furthermore, compared to that in the P(HG) group, collagen IV protein expression was significantly lower in the P(HG+ATX) group. The *in vitro* results of our study suggested that the diabetic microenvironment caused autophagy and fibrosis in HMCs, and this phenomenon could be ameliorated by ATX. These data also support the emerging notion that molecular signaling crosstalk exists between autophagic podocytes and mesangial cells.

4. Discussion

Nutritional strategies for treating fibrosis are currently a growing area of research, and several natural substances exhibit effective antifibrotic effects. Recent studies have indicated that ATX can reduce organ fibrosis, including fibrosis in the liver, heart, lungs, and kidneys, suggesting that ATX represents a promising treatment for fibrosis. The kidneys are particularly susceptible to the development of fibrotic damage, often as a result of chronic conditions such as unilateral ureteral obstruction (UUO) and DN [26]. However, the effect of ATX on DN remains unclear. In this study, we found that α -SMA and collagen IV expression decreased in the kidneys of diabetic rats after ATX treatment. Similar results were observed *in vitro* in podocytes. Therefore, these results indicate that podocytes are the target cells of ATX.

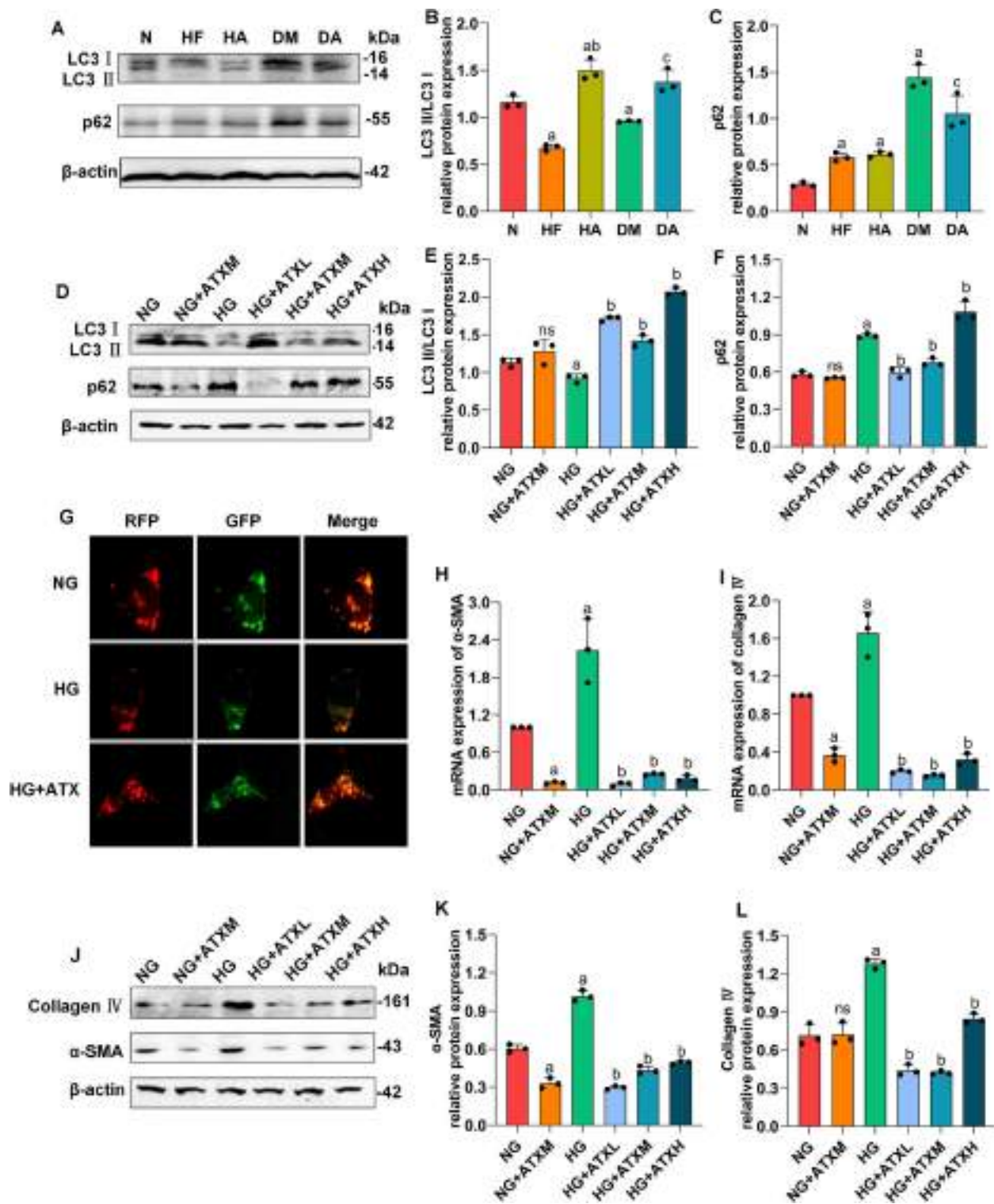


Figure 3. Astaxanthin regulates proteins related to autophagy in the kidneys of rats and podocytes. (A, B, C) LC3II/I and p62 protein expression levels in the kidney were determined using Western blotting. (D, E, F) LC3II/LC3I and p62 protein expression in podocytes determined using Western blotting. (G) measurement of autophagic flux by using RFP-GFP-LC3 (original magnification, $\times 400$) in podocytes. (H, I) α -SMA and collagen IV mRNA expression in podocytes was determined using real-time PCR. (J, K, L) α -SMA and collagen IV protein expression in podocytes determined using Western blotting. The results are presented as the mean \pm SD, $n \geq 3$. $^a p < 0.05$, $^{ns} p > 0.05$ compared with the N group, $^b p < 0.05$ compared with the HF group, $^c p < 0.05$ compared with the DM group; $^a p < 0.05$ compared with the NG group, $^b p < 0.05$ compared with the HG group.

Thus, the question of how ATX is regulated in DN fibrosis arises. Autophagy plays a central role in several diseases, including cancer, pathogenic infections, and metabolic diseases. Autophagy inducers are currently receiving

considerable attention, as both the induction and inhibition of autophagy may be beneficial. LC3 has been proposed to be an indicator of self-phagocytosis. There are two types of LC3: LC3-I, which is generally present in the cytosol, and LC3-II,

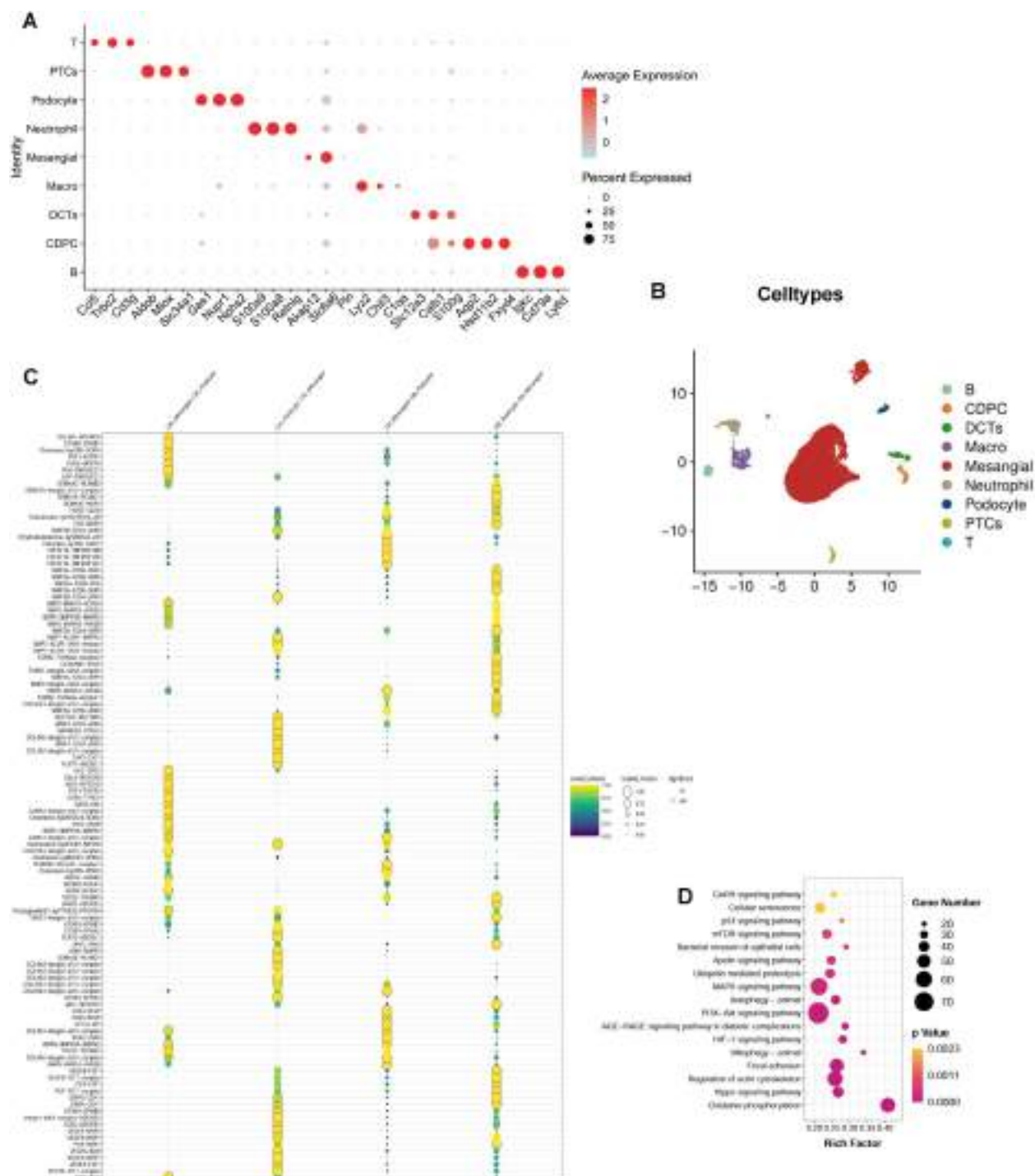


Figure 4. Communication networks in podocytes and mesangial cells in diabetic nephropathy. (A) cell markers of different cells. (B) t-SNE plot demonstrating different cell types in the DN. (C) ligand-receptor pairs in different cell types. (D) pathway enrichment analysis of podocytes in the DN.

which is present in the membrane. LC3-II is an insoluble protein that can be easily broken down by combining LC3-I with phosphatidylethanolamine [27,28]. During autophagy, LC3-I is cleaved and converted to LC3-II, which translocates to the autophagosomal membrane, leading to autophagosome formation. Therefore, the degree of cellular autophagic activity can be judged by the magnitude of the LC3-II/LC3-I ratio [29]. p62, an important autophagy receptor, is negatively correlated with the number of autophagic lysosomes. p62 also plays a

vital role in the regulation of intracellular signaling [30]. Autophagy is considered an important regulatory factor for myofibroblast differentiation, tissue remodeling, and fibrogenesis [31]. Previous studies have shown an interaction between autophagy and DN fibrosis [32,33]. In the kidney, indirect evidence from experiments with well-known autophagy inducers also suggested that autophagy has protective effects during DN development [34,35]. A study revealed a significant reduction in autophagy levels in the kidney tissue of DN rats, as

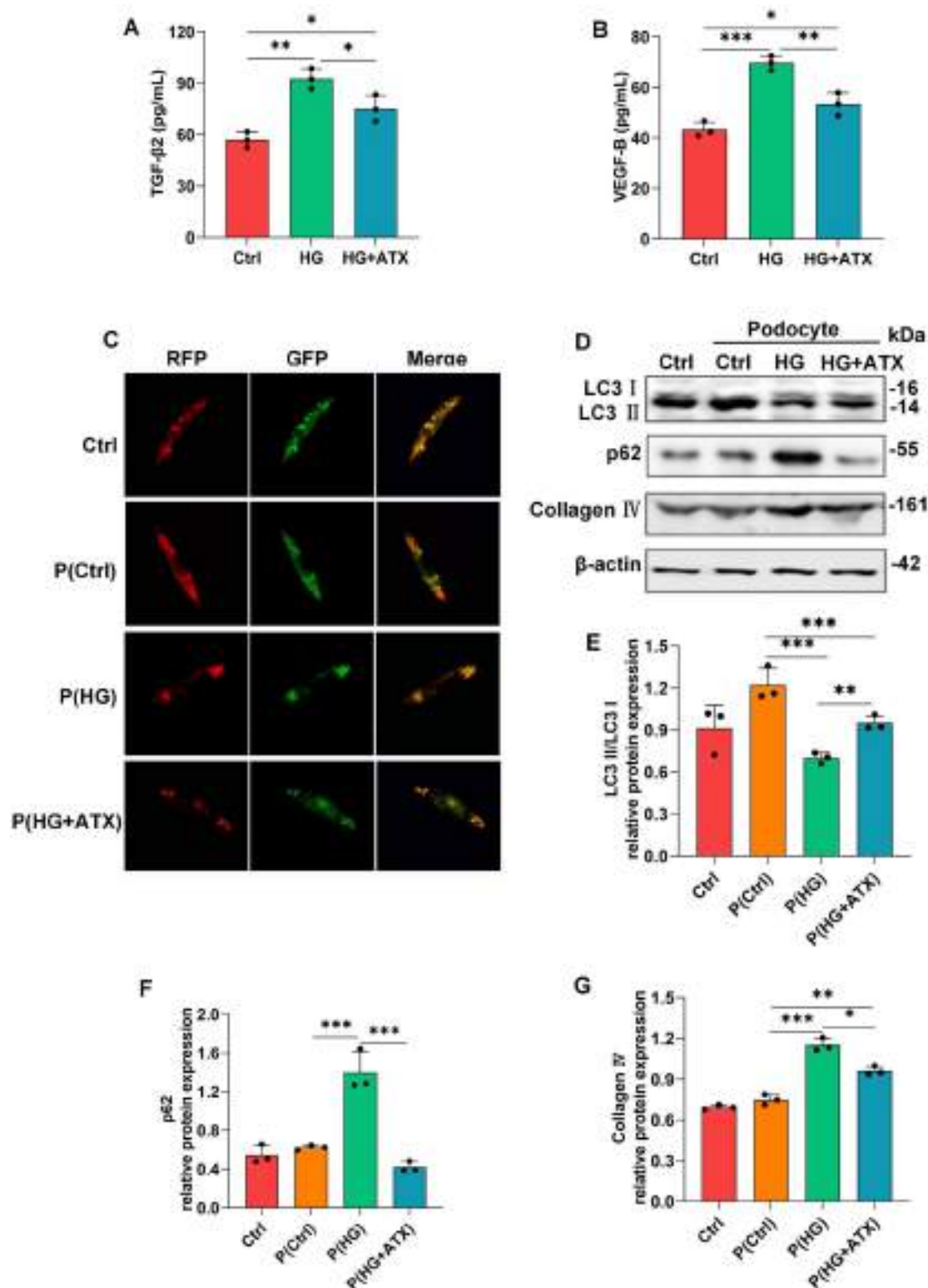


Figure 5. Podocyte autophagy results in the secretion of factors into the supernatants that affect mesangial cell autophagy. (A, B) VEGF-B and TGF-β levels were determined using ELISA. (C) measurement of autophagic flux by using RFP-GFP-LC3 (original magnification, $\times 400$) in HMCs. (D, E, F, G) LC3II/LC3I, p62 and collagen IV protein expression in HMCs determined using Western blotting. The results are presented as the mean \pm SD, $n \geq 3$. $*p < 0.05$, $**p < 0.01$, $***p < 0.001$.

indicated by an increase in p62 protein levels and a notable decrease in LC3 expression [36]. Another study also revealed that autophagy defects were distinct in the kidney tissue of

DN mice and that enhancing autophagy in kidney cells may improve the disease status of DN [37]. Therefore, we suggest that the activation of autophagy can help patients resist

fibrosis and delay DN progression. Podocyte damage has been regarded as the focus of research to decipher the cellular and molecular mechanisms of DN [6]. Podocyte damage is always accompanied by a decrease in autophagy flux, p62 accumulation, and the interaction between p62 and LC3 [38,39]. To investigate whether hyperglycemia leads to renal autophagy dysfunction, we initially examined LC3 and p62 expression in podocytes under hyperglycemic conditions. LC3-II and p62 protein levels were examined in this study to monitor autophagy and autophagic flux. In this study, LC3 expression in diabetic and high-fat kidneys was significantly lower than that in the control group, and p62 expression was significantly greater in diabetic and high-fat kidneys compared with the control group. However, ATX upregulated autophagy in the DM group. Previous studies have demonstrated that the autophagic activity of podocytes decreases after diabetes induction by STZ [40]. *In vitro*, autophagy and its associated proteins were decreased in cultured podocytes exposed to high concentrations of glucose [40,41]. In the present study, we observed that high glucose inhibited autophagy in podocytes, but ATX upregulated autophagy in podocytes, as evidenced by enhanced LC3-II levels and attenuated p62 levels with a reduced number of autophagosomes. The findings of the current study and those of previous reports indicate that autophagy can also be affected by high glucose levels in podocytes and that ATX may inhibit the activation of these cells by increasing autophagy levels. Moreover, our findings showed that diabetic rats and podocytes cultured in high glucose conditions exhibited markedly increased α -SMA and collagen IV expression; however, ATX treatment reversed this effect. These data suggest that ATX might play a role in upregulating the autophagy signaling pathway, which indirectly leads to a reduction in α -SMA and collagen IV expression.

Abnormalities in podocytes and mesangial cells play a key role in DN development. Crosstalk between mesangial cells and podocytes promotes DN development. Studies have shown that endothelial cells and podocytes in the filtration barrier directly interact with the glomerular basement membrane (GBM) in a hyperglycemic environment or regulate mesangial cells through crosstalk to promote DN progression [42]. In the pathological condition of hyperglycemia, the activation of intracellular signaling molecules leads to dysregulation of vascular growth factors, including VEGF and TGF- β , which are involved in regulating abnormal angiogenesis and eventually albuminuria [43]. An article showed that reducing VEGF-B signaling could ameliorate glomerular lipotoxicity and, consequently, DN progression [44]. Another study showed that overactivation of the TGF- β signaling pathway in a high-glucose environment harms mesangial cells, podocytes, and endothelial cells [45]. Our findings showed that VEGF-B and TGF- β secretion into the supernatant of podocytes increased under high glucose conditions. When the supernatant was transferred to HMCs, autophagy decreased. However, in the supernatant of ATX-treated podocytes, the secretion of pathological crosstalk factors in podocytes

and the upregulation of HMC autophagy was inhibited, thereby reducing fibrosis in HMCs.

5. Conclusion

Our study demonstrated that ATX upregulated autophagic activity in podocytes, which may mediate the renoprotective effects induced by DN. Furthermore, crosstalk between podocytes and HMCs potentially causes renal injury in diabetes. However, ATX treatment reversed this phenomenon. From a clinical utility standpoint, this research holds promise for addressing renal fibrosis in DN through oral treatment, thus reducing the medical burden and simultaneously increasing economic benefits.

Acknowledgments

The authors would like to acknowledge Ningbo University for their material support for this project. We acknowledge the 'Chen Zhengyue. 2018. Astaxanthin Attenuates Diabetic Kidney Injury Through Up-Regulation of Autophagy. Kidney week 2018 Abstract. The American Society of Nephrology. TH-PO865 (Page 345)' poster presentation.

Authors' contributions

Mengqi Hong developed the study concept and design. Zhenyue Chen and Beiyan Bao developed the methodology and wrote, reviewed, and revised the paper. Zhenyu Nie provided data acquisition, data analysis and interpretation, and statistical analysis. All the authors have read and approved the final paper.

Disclosure statement

The authors declare that there are no conflicts of interest.

Funding

This work was supported by the Natural Science Foundation of Ningbo Municipality (2021J024) and the Ningbo Health Science and Technology Plan Project (2023Y40).

Data availability statement

The analyzed data are available from the corresponding author upon reasonable request.

References

- [1] Ritz E, Orth SR. Nephropathy in patients with type 2 diabetes mellitus. *N Engl J Med*. 1999;341(15):1127–1133. doi: [10.1056/NEJM199910073411506](https://doi.org/10.1056/NEJM199910073411506).
- [2] Saran R, Li Y, Robinson B, et al. US renal data system 2014 annual data report: epidemiology of kidney disease in the United States. *Am J Kidney Dis*. 2015;66(1 Suppl 1):Svii, S1–305. doi: [10.1053/j.ajkd.2015.05.001](https://doi.org/10.1053/j.ajkd.2015.05.001).

- [3] Yang W, Lu J, Weng J, et al. Prevalence of diabetes among men and women in China. *N Engl J Med*. 2010;362(12):1090–1101. doi: [10.1056/NEJMoa0908292](https://doi.org/10.1056/NEJMoa0908292).
- [4] Xu Y, Wang L, He J, et al. Prevalence and control of diabetes in Chinese adults. *JAMA*. 2013;310(9):948–959. doi: [10.1001/jama.2013.168118](https://doi.org/10.1001/jama.2013.168118).
- [5] Zhang L, Wang F, Wang L, et al. Prevalence of chronic kidney disease in China: a cross-sectional survey. *Lancet*. 2012;379(9818):815–822. doi: [10.1016/S0140-6736\(12\)60033-6](https://doi.org/10.1016/S0140-6736(12)60033-6).
- [6] Barutta F, Bellini S, Gruden G. Mechanisms of podocyte injury and implications for diabetic nephropathy. *Clin Sci (Lond)*. 2022;136(7):493–520. doi: [10.1042/CS20210625](https://doi.org/10.1042/CS20210625).
- [7] Li X, Zhang Y, Xing X, et al. Podocyte injury of diabetic nephropathy: novel mechanism discovery and therapeutic prospects. *Biomed Pharmacother*. 2023;168:115670. doi: [10.1016/j.biopha.2023.115670](https://doi.org/10.1016/j.biopha.2023.115670).
- [8] Dimke H, Maezawa Y, Quaggin SE. Crosstalk in glomerular injury and repair. *Curr Opin Nephrol Hypertens*. 2015;24(3):231–238. doi: [10.1097/MNH.0000000000000117](https://doi.org/10.1097/MNH.0000000000000117).
- [9] Nikolettou V, Markaki M, Palikaras K, et al. Crosstalk between apoptosis, necrosis and autophagy. *Biochim Biophys Acta*. 2013;1833(12):3448–3459. doi: [10.1016/j.bbamcr.2013.06.001](https://doi.org/10.1016/j.bbamcr.2013.06.001).
- [10] Lin Q, Banu K, Ni Z, et al. Podocyte autophagy in homeostasis and disease. *J Clin Med*. 2021;10(6):1184. doi: [10.3390/jcm10061184](https://doi.org/10.3390/jcm10061184).
- [11] Kume S, Thomas MC, Koya D. Nutrient sensing, autophagy, and diabetic nephropathy. *Diabetes*. 2012;61(1):23–29. doi: [10.2337/db11-0555](https://doi.org/10.2337/db11-0555).
- [12] Teh YM, Mualif SA, Lim SK. A comprehensive insight into autophagy and its potential signaling pathways as a therapeutic target in podocyte injury. *Int J Biochem Cell Biol*. 2022;143:106153. doi: [10.1016/j.biocel.2021.106153](https://doi.org/10.1016/j.biocel.2021.106153).
- [13] Chang MX, Xiong F. Astaxanthin and its effects in inflammatory responses and inflammation-associated diseases: recent advances and future directions. *Molecules*. 2020;25(22):5342. doi: [10.3390/molecules25225342](https://doi.org/10.3390/molecules25225342).
- [14] Kohandel Z, Farkhondeh T, Aschner M, et al. Anti-inflammatory action of astaxanthin and its use in the treatment of various diseases. *Biomed Pharmacother*. 2022;145:112179. doi: [10.1016/j.biopha.2021.112179](https://doi.org/10.1016/j.biopha.2021.112179).
- [15] Wu L, Mo W, Feng J, et al. Astaxanthin attenuates hepatic damage and mitochondrial dysfunction in non-alcoholic fatty liver disease by up-regulating the FGF21/PGC-1 α pathway. *Br J Pharmacol*. 2020;177(16):3760–3777. doi: [10.1111/bph.15099](https://doi.org/10.1111/bph.15099).
- [16] Islam MA, Al Mamun MA, Faruk M, et al. Astaxanthin ameliorates hepatic damage and oxidative stress in carbon tetrachloride-administered rats. *Pharmacognosy Res*. 2017;9(Suppl 1):S84–S91. doi: [10.4103/pr.pr_26_17](https://doi.org/10.4103/pr.pr_26_17).
- [17] Si P, Zhu C. Biological and neurological activities of astaxanthin (Review). *Mol Med Rep*. 2022;26(4):300. doi: [10.3892/mmr.2022.12816](https://doi.org/10.3892/mmr.2022.12816).
- [18] Pereira CPM, Souza ACR, Vasconcelos AR, et al. Antioxidant and anti-inflammatory mechanisms of action of astaxanthin in cardiovascular diseases (Review). *Int J Mol Med*. 2021;47(1):37–48. doi: [10.3892/ijmm.2020.4783](https://doi.org/10.3892/ijmm.2020.4783).
- [19] Zhuge F, Ni Y, Wan C, et al. Anti-diabetic effects of astaxanthin on an STZ-induced diabetic model in rats. *Endocr J*. 2021;68(4):451–459. doi: [10.1507/endocrj.EJ20-0699](https://doi.org/10.1507/endocrj.EJ20-0699).
- [20] Landon R, Gueguen V, Petite H, et al. Impact of astaxanthin on diabetes pathogenesis and chronic complications. *Mar Drugs*. 2020;18(7):357. doi: [10.3390/md18070357](https://doi.org/10.3390/md18070357).
- [21] Chen H, Wang J, Li R, et al. Astaxanthin attenuates pulmonary fibrosis through IncITP and mitochondria-mediated signal pathways. *J Cell Mol Med*. 2020;24(17):10245–10250. doi: [10.1111/jcmm.15477](https://doi.org/10.1111/jcmm.15477).
- [22] Shen M, Chen K, Lu J, et al. Protective effect of astaxanthin on liver fibrosis through modulation of TGF- β 1 expression and autophagy. *Mediators Inflamm*. 2014;2014:954502–954514. doi: [10.1155/2014/954502](https://doi.org/10.1155/2014/954502).
- [23] Mogensen CE. Microalbuminuria as a predictor of clinical diabetic nephropathy. *Kidney Int*. 1987;31(2):673–689. doi: [10.1038/ki.1987.50](https://doi.org/10.1038/ki.1987.50).
- [24] Miaomiao W, Chunhua L, Xiaochen Z, et al. Autophagy is involved in regulating VEGF during high-glucose-induced podocyte injury. *Mol Biosyst*. 2016;12(7):2202–2212. doi: [10.1039/c6mb00195e](https://doi.org/10.1039/c6mb00195e).
- [25] Marcelin G, Da Cunha C, Gamblin C, et al. Autophagy inhibition blunts PDGFRA adipose progenitors' cell-autonomous fibrogenic response to high-fat diet. *Autophagy*. 2020;16(12):2156–2166. doi: [10.1080/15548627.2020.1717129](https://doi.org/10.1080/15548627.2020.1717129).
- [26] Li K, Wang W, Xiao W. Astaxanthin: a promising therapeutic agent for organ fibrosis. *Pharmacol Res*. 2023;188:106657. doi: [10.1016/j.phrs.2023.106657](https://doi.org/10.1016/j.phrs.2023.106657).
- [27] Song T, Su H, Yin W, et al. Acetylation modulates LC3 stability and cargo recognition. *FEBS Lett*. 2019;593(4):414–422. doi: [10.1002/1873-3468.13327](https://doi.org/10.1002/1873-3468.13327).
- [28] Wu YY, Zheng BR, Chen WZ, et al. Expression and role of autophagy related protein p62 and LC3 in the retina in a rat model of acute ocular hypertension. *Int J Ophthalmol*. 2020;13(1):21–28. doi: [10.18240/ijo.2020.01.04](https://doi.org/10.18240/ijo.2020.01.04).
- [29] Ma R, He Y, Fang Q, et al. Ferulic acid ameliorates renal injury via improving autophagy to inhibit inflammation in diabetic nephropathy mice. *Biomed Pharmacother*. 2022;153:113424. doi: [10.1016/j.biopha.2022.113424](https://doi.org/10.1016/j.biopha.2022.113424).
- [30] Klionsky DJ, Abdelmohsen K, Abe A, et al. Guidelines for the use and interpretation of assays for monitoring autophagy. *Selliez, Iban. Autophagy*. 2016;12(1):1–222. doi: [10.1080/15548627.2015.1100356](https://doi.org/10.1080/15548627.2015.1100356).
- [31] Liang S, Wu YS, Li DY, et al. Autophagy and renal fibrosis. *Aging Dis*. 2022;13(3):712–731. doi: [10.14336/AD.2021.1027](https://doi.org/10.14336/AD.2021.1027).
- [32] Chen Z, Liang H, Yan X, et al. Astragalus polysaccharide promotes autophagy and alleviates diabetic nephropathy by targeting the lncRNA Gm41268/PRLR pathway. *Ren Fail*. 2023;45(2):2284211. doi: [10.1080/0886022X.2023.2284211](https://doi.org/10.1080/0886022X.2023.2284211).
- [33] Su PP, Liu DW, Zhou SJ, et al. Down-regulation of Risa improves podocyte injury by enhancing autophagy in diabetic nephropathy. *Mil Med Res*. 2022;9(1):23. doi: [10.1186/s40779-022-00385-0](https://doi.org/10.1186/s40779-022-00385-0).
- [34] Komatsu M, Waguri S, Koike M, et al. Homeostatic levels of p62 control cytoplasmic inclusion body formation in autophagy-deficient mice. *Cell*. 2007;131(6):1149–1163. doi: [10.1016/j.cell.2007.10.035](https://doi.org/10.1016/j.cell.2007.10.035).
- [35] Li X, Zhu Q, Zheng R, et al. Puerarin attenuates diabetic nephropathy by promoting autophagy in podocytes. *Front Physiol*. 2020;11:73. doi: [10.3389/fphys.2020.00073](https://doi.org/10.3389/fphys.2020.00073).

- [36] Jiang Y, Zhao Y, Zhu X, et al. Effects of autophagy on macrophage adhesion and migration in diabetic nephropathy. *Ren Fail.* 2019;41(1):682–690. doi: [10.1080/0886022X.2019.1632209](https://doi.org/10.1080/0886022X.2019.1632209).
- [37] Zhang P, Fang J, Zhang J, et al. Curcumin inhibited podocyte cell apoptosis and accelerated cell autophagy in diabetic nephropathy via regulating Beclin1/UVRAG/Bcl2. *Diabetes Metab Syndr Obes.* 2020;13:641–652. doi: [10.2147/DMSO.S237451](https://doi.org/10.2147/DMSO.S237451).
- [38] Han YP, Liu LJ, Yan JL, et al. Autophagy and its therapeutic potential in diabetic nephropathy. *Front Endocrinol (Lausanne).* 2023;14:1139444. doi: [10.3389/fendo.2023.1139444](https://doi.org/10.3389/fendo.2023.1139444).
- [39] Jin J, Shi Y, Gong J, et al. Exosome secreted from adipose-derived stem cells attenuates diabetic nephropathy by promoting autophagy flux and inhibiting apoptosis in podocyte. *Stem Cell Res Ther.* 2019;10(1):95. doi: [10.1186/s13287-019-1177-1](https://doi.org/10.1186/s13287-019-1177-1).
- [40] Guo H, Wang Y, Zhang X, et al. Astragaloside IV protects against podocyte injury via SERCA2-dependent ER stress reduction and AMPK α -regulated autophagy induction in streptozotocin-induced diabetic nephropathy. *Sci Rep.* 2017;7(1):6852. doi: [10.1038/s41598-017-07061-7](https://doi.org/10.1038/s41598-017-07061-7).
- [41] Audzeyenka I, Rogacka D, Piwkowska A, et al. Viability of primary cultured podocytes is associated with extracellular high glucose-dependent autophagy downregulation. *Mol Cell Biochem.* 2017;430(1–2):11–19. doi: [10.1007/s11010-017-2949-5](https://doi.org/10.1007/s11010-017-2949-5).
- [42] Fu J, Lee K, Chuang PY, et al. Glomerular endothelial cell injury and cross talk in diabetic kidney disease. *Am J Physiol Renal Physiol.* 2015;308(4):F287–F297. doi: [10.1152/ajprenal.00533.2014](https://doi.org/10.1152/ajprenal.00533.2014).
- [43] Forbes JM, Fukami K, Cooper ME. Diabetic nephropathy: where hemodynamics meets metabolism. *Exp Clin Endocrinol Diabetes.* 2007;115(2):69–84. doi: [10.1055/s-2007-949721](https://doi.org/10.1055/s-2007-949721).
- [44] Falkevall A, Mehlem A, Palombo I, et al. Reducing VEGF-B signaling ameliorates renal lipotoxicity and protects against diabetic kidney disease. *Cell Metab.* 2017;25(3):713–726. doi: [10.1016/j.cmet.2017.01.004](https://doi.org/10.1016/j.cmet.2017.01.004).
- [45] McGinn S, Poronnik P, King M, et al. High glucose and endothelial cell growth: novel effects independent of autocrine TGF- β 1 and hyperosmolarity. *Am J Physiol Cell Physiol.* 2003;284(6):C1374–C1386. doi: [10.1152/ajp-cell.00466.2002](https://doi.org/10.1152/ajp-cell.00466.2002).